Peer-reviewed version available at Membranes 2018, 8, 128; doi:10.3390/membranes8040128

Study of the effect of inorganic particles on the gas transport properties of glassy polyimides for selective CO_2 and H_2O separation

Sara Escorihuela[1,2], Lucía Valero[1,2], Alberto Tena[2*], Sergey Shishatskiy[2*], Sonia Escolástico[1], Torsten Brinkmann[2], Jose Manuel Serra[1*]

[1]Instituto de Tecnología Química, Universitat Politècnica de València-Consejo Superior de Investigaciones Científicas, Avda. Los Naranjos, s/n, 46022, Valencia, Spain

[2]Helmholtz-Zentrum Geesthacht, Institute of Polymer Research, Max-Planck-Str.1, 21502 Geesthacht, Germany

Corresponding authors: alberto.tena@hzg.de; sergey.shishatskiy@hzg.de; jmserra@itq.upv.es

Abstract

Three polyimides and six inorganic fillers in a form of nanometer-sized particles were studied as thick film solution cast mixed matrix membranes (MMMs) for transport of CO_2, CH_4 and H_2O. Gas transport properties and electron microscopy images indicate good polymer-filler compatibility for all membranes. The only filler type which demonstrated good distribution throughout the membrane thickness at 10 wt. % loading was $BaCe_{0.2}Zr_{0.7}Y_{0.1}O_3$ (BCZY). The influence of this filler on MMM gas transport properties was studied in detail for 6FDA-6FpDA in a filler content range from 1 to 20 wt.% and for Matrimid® and P84® at 10 wt. % loading. The most promising result was obtained for Matrimid® - 10wt% BCZY MMM, which showed improvement in CO_2 and H_2O permeabilities accompanied by increased CO_2/CH_4 selectivity and high water selective membrane at elevated temperatures without H_2O/permanent gas selectivity loss.

Introduction

Mixed matrix membranes (MMMs) [1, 2] are considered as a very promising route to overcome limitations of the Robeson upper bound of the permeability/selectivity relationship by combining good mechanical but rather disappointing gas transport properties of polymers with excellent diffusion and sorption properties of inorganic porous media having very poor mechanical properties, *e.g.* flexibility [3].

Gas separation membranes have been on the market since 1980 [4] and have proven their reliability [5]. Unfortunately, since the boom of membranes introduction into the market at the end of the 20th century, not too many new membranes reached practical application. The reason for it lays in the versatility of existing membranes that allow to combine membrane separation stages with other unit operations and to achieve goals of the separation process [6]. New

Peer-reviewed version available at Membranes 2018, 8, 128; doi:10.3390/membranes8040128

membranes introduced to the market should exhibit properties significantly better compared to those already commercially available. At this point, the combination of properties of polymers and inorganic substances able to selectively transport gas or vapor molecules becomes very appealing [7].

The requirements for polymers to be used in membranes are: adequate gas transport properties (balance between permeability and selectivity), processability as a thin film, good mechanical properties, and stability of properties as a function of time and high reproducible manufacturing from batch to batch. For the formation of MMMs, good adhesion between the polymer matrix and the inorganic filler is essential, especially in case of polymers with high T_g [8].

The inorganic fillers to be used in MMMs should have (i) particles as small as possible since selective layers of modern polymer based gas separation membranes have a thickness of 100 nm and less; (ii) good affinity to the polymer; and (iii) gas transport properties matching, for the target gas in the separation process, those of the matrix polymer [9].

Depending on the compatibility of the filler and the polymer matrix, four different cases (Figure 1) and the expected effect on the separation properties can be described [10-14]. Case 1 is an ideal situation, where the filler is perfectly incorporated into the polymer matrix. This situation can result in an improvement of the separation properties of the mixed matrix material. In Case 2, there is a rigidification of the polymer matrix in the area around the filler. This normally results in an increase of the selectivity, due to the increased rigidity, but also in a decrease of the permeability. This is normally confirmed by an increase on the T_g of the MMMs. Case 3 exhibits a creation of an interphase due to the incompatibility between the particle and the polymer matrix. This results in an increase of the permeability due to the bigger fractional free volume but also in a decrease of the selectivity. In Case 4, the polymer matrix penetrates the pore or free volume of the filler. In this case both, permeability and selectivity decrease.

In this work, several MMMs were studied for gas transport properties with focus on CO_2, CH_4 and H_2O as components in various industrially relevant gas mixtures as *e.g.* natural gas, biogas as well as gas streams in chemical and petrochemical industries [15-18]. Biogas and natural gas are considered as most environmentally friendly resources for large scale electric energy production and as sources with significant methane content, which is involved in several relevant reactions such as combustion, steam reforming or halogenation. For example, in Germany, natural gas contains about 95% CH_4 and not more than 2% CO_2 concentration in the gas pipelines [19-21]. On the other hand, biogas is a mixture of several gases produced by the anaerobic decomposition of organic matter. Biogas mainly consists of methane (50-70%), carbon dioxide (30-50%), and other compounds including hydrogen sulfide (H_2S), water, and other trace gas compounds [22]. The membranes considered in this study could be used to separate CO_2 from these gases.

Peer-reviewed version available at Membranes 2018, 8, 128; doi:10.3390/membranes8040128

Additionally, these membranes could also be applied to remove water at low temperature in several combustion processes, in order to recover it and on-site reuse for other purposes.

In the current study, three polyimides and six inorganic fillers were used to prepare MMMs as thick films and the corresponding gas transport properties for CO_2, CH_4 and H_2O were systematically studied. Polyimides were selected due to their outstanding gas transport properties for several gas pairs as CO_2/CH_4 or O_2/N_2 and, in case of studied polymers, excellent film forming properties. The six inorganic materials used as nano-sized particles were selected taking into account the expected good affinity for gas molecules as CO_2 and water vapour [23].

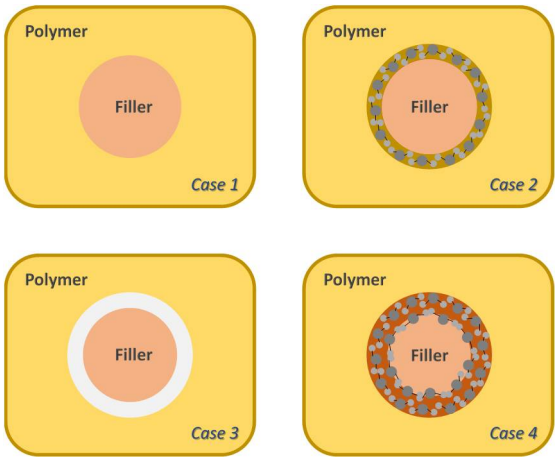

Figure 1. Schematic diagram of various structures for MMMs

Experimental section

1. Materials

Polymers

Three different polyimides were employed in the present study: 6FDA-6FpDA, Matrimid® 5218 and P84®. The 6FDA-6FpDA polyimide was synthesized following the classical *in-situ* silylation two steps method [24]. A detailed description of this synthesis can be found in a previous work [25]. Polyimides P84® and Matrimid® 5218 were purchased from HP Polymer GmbH (Austria) and Huntsman Advanced Materials (USA), respectively.

Solvents

Tetrahydrofuran (THF), N-methyl-2-pyrrolidon (NMP), dimethylformamide (DMF), dimethylacetamid (DMAc), toluene, chloroform, and isopropanol for analysis grade were purchased from Merck (Germany) and used as received.

Particles

Preprints (www.preprints.org) | NOT PEER-REVIEWED | Posted: 8 November 2018 doi:10.20944/preprints201811.0186.v1

Peer-reviewed version available at Membranes 2018, 8, 128; doi:10.3390/membranes8040128

Six inorganic fillers were employed: 8mol% Yttria Stabilized Zirconia (8YSZ), La_2O_3, $La_{5.4}WO_{12}$ (LaWO), $BaCe_{0.2}Zr_{0.7}Y_{0.1}O_3$ (BCZY) and two zeolites (ITQ-2 and Beta). 8YSZ powder was provided by Tosoh Corporation (Japan). La_2O_3 was synthesized by co-precipitation from lanthanum nitrate ($La(NO_3)_3$) and subsequent calcination at 800 °C for 5 h. LaWO, provided by CerPoTech (Norway) in powder form was calcined at 800 °C for 6 h. BCZY powder, also provided by CerPoTech, was calcined at 950 °C for 6h. Nanocrystalline Beta zeolite (BEA material) and ITQ-2 (delaminated MCM-22 zeolite material) [26] were synthesized by the ITQ and are here used after calcination (organics removal) in its acidic form. All the fillers were ball-milled previously for 24 hours. Table 1 shows a summary of the fillers properties.

Table 1: Properties of the used particles. 8YSZ [27], La_2O_3 [28], LaWO [29], BCZY [30, 31], ITQ-2 [26] and Beta [32].

PARTICLES	8YSZ	La2O3	LaWO	BCZY	ITQ-2	Beta
Description	8% mol of Y_2O_3 stabilized ZrO_2 (Tosoh)	Co-precipitation from $La(NO_3)_3$. Calcined 800 °C/5h	$La_{5.4}WO_{12}$ (CerPoTech). Calcined 950 °C/6h	$BaCe_{0.2}Zr_{0.7}Y_{0.1}O_3$ (CerPoTech). Calcined 950 °C/6h	ITQ-2 zeolite. Si/Al = 50	Zeolite nanocrystalline. Si/Al = 12.5
Structure	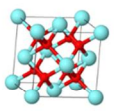	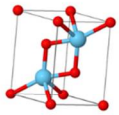	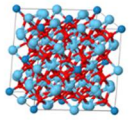	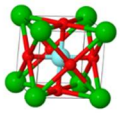		
Density (g/cm^3)	5.95	6.56	6.58	6.14	-	-
BET area (m^2/g)	6.0	2.9	9.4	31.4	>700	>700
Size (nm)	20-80	60-100	30-120	30-100	Thin sheets (2.5 thick)	10-30
Uses	Solid electrolyte in solid oxide fuel cells (SOFC)	Ferroelectric materials and as feedstock for catalysts	Asymmetric membranes for hydrogen separation	Electrolyte material for proton-conducting fuel cells (PCFC)	Catalysis	Catalysis

2. Membranes fabrication

Inorganic particles dispersion

Different solvents such as THF, NMP, DMF, DMAc, toluene, chloroform, and isopropanol were tested for the dispersion of the particles. The ultrasonic devices used to disperse the fillers were the digital Sonifier®, models 250 & 450 (BRANSON Ultrasonics Corporation). The dispersion was carried out with the pulse/pause mode, in particular, pulse off for one second and pulse on for one second for a total duration of 30 minutes. In addition, the dissolution container was inside an ice bath to avoid the sample heating during the dispersion process. In all the cases, the best dispersions and the most visually stable over time (smallest degree of sedimentation) were

obtained by using NMP. The zeolites were fully suspended whereas in the dispersions obtained with 8YSZ, La_2O_3, LaWO and BCZY some sedimentation with time was observed.

Membranes formation

Mix matrix membranes (MMMs) were made with 250 mg of polymer and inorganic fillers and 2.25 g of solvent. First, the inorganic fillers were dried at 120 °C for 24 h before the membrane preparation. Then, the fillers were dispersed in 1 g of NMP, as a solvent, by using an ultrasound device. At the same time, the polymer was dissolved with the rest of the solvent. The particle suspension was finally added to the polymer solution, obtaining a homogeneous solution of polymer and fillers. Subsequently, membranes were prepared by following the solvent evaporation method. The mixed matrix solutions were poured into metal rings placed on a heating plate at 70 °C for 12h. Then, the membranes were heat treated following the steps: (a) 100 °C under vacuum for 1.5 h, (b) 200 °C under vacuum for 2 h and (c) cooling to room temperature under vacuum.

3. Samples characterization

Thermogravimetric analysis (TGA) experiments were carried out on the thermal analysis instrument NETZSCH TG 209 F1 Iris in order to evaluate the thermal stability of the MMM and quantify the percentage of fillers. Disc samples with weights of between 5 and 15 mg were cut from the pieces obtained as described in section 2.2. The TGA experiments consisted of two steps: (i) first, the sample was heated from 30 °C to 800 °C at 10 °C/min under an argon flow (dynamic scan); (ii) once 800 °C were reached, the temperature was maintained for 30 minutes under synthetic air (static scan), in order to burn out the organic from the samples.

The apparent molecular weight of the polymers and the MMMs was determined by Gel permeation Chromatography (GPC) after calibration with polystyrene standards. GPC measurements were performed at 40 °C having DMAc as eluent on a Waters instrument (Waters GmbH, Eschborn, Germany) equipped with polystyrene gel columns of different pore sizes, using a refractive index (RI) detector.

The XRD analysis were performed by using a D8 DISCOVER X-ray diffractometer (Bruker). The range of measured Bragg angles was from 2 to 82°, with an increase of 10°. A 50 kV voltage and 1000 μA current was used.

The morphology of prepared MMMs and particle distribution throughout the membrane cross-section were analyzed using a scanning electron microscope “Merlin” (Zeiss, Oberkochen, Germany). Samples for cross-sectional images were prepared by breaking the membrane immersed into liquid nitrogen and subsequent coating with a 4 nm carbon layer.

The permeability, diffusivity and solubility coefficients of CH_4, CO_2 and H_2O vapor in the manufactured membranes were determined by using the well-known constant volume, variable

pressure method, *i.e.* the "time-lag method" [24]. The basic principle is the measurement of the transitory response at the downstream part of a membrane to a pressure step at the upstream part, that is, the time-lag (t_0). The diffusion coefficient (D) is linked to the time-lag (t_0) through the Equation (1).

$$t_0 = \frac{l^2}{6 \cdot D} \quad (1)$$

where l is the thickness of the membrane. The permeability coefficient (P) can be obtained from the range where the permeate pressure increases linearly (Equation 2).

$$P = D \cdot S = \frac{V_p l (p_{p2} - p_{p1})}{ART\Delta t(p_f - (p_{p2} + p_{p1})} \quad (2)$$

where V_p is the constant permeate volume, l is the film thickness, A is the effective area of the membrane, R is the gas constant, Δt is the time of the permeate pressure increase from p_{p1} to p_{p2}, p_f is the feed pressure. Finally, solubility coefficient (S) can be obtained with the permeability and the diffusion coefficient by means of Equation 3.

$$S = \frac{P}{D} \quad (2)$$

The measurements were made at different temperatures and at 1 bar of feed pressure. For each gas measurement, the facility was evacuated until no desorption from the membrane was observed and the gas to be measured was subsequently refilled. The feed and permeate sides of the membrane are connected to a vacuum pump with valves and additional valves connect the feed side with several gases.

Experiments on water vapor transport were carried out as follows: The pressure vessel keeping feed pressure of a gas or vapor under study at a constant level during the acquisition of the time-lag curve was filled with water vapor corresponding to the saturation pressure at a given temperature. For the beginning of the experiment, the feed pressure vessel was connected to the previously evacuated measurement cell by opening vacuum valves. It caused a drop of the vapor pressure to approximately 70 % of vapor activity at a given temperature. Due to the design of the vacuum system of the "time-lag" facility it is not possible to carry out vapor measurements at activities higher than 70%. After the time-lag curve was recorded the system was completely evacuated and experiment repeated for 3 times. For the CH_4 and CO_2, gas properties were studied at temperatures up to 80 ºC.

Results and Discussion

1. Thermal properties

Thermogravimetric analysis experiments (TGA) were performed in order to evaluate the thermal stability of the MMMs and to additionally determine the real amount of particles in the final sample [33]. The parameter used to evaluate the quantity of particles in the membranes is the residual mass (R_M). In Table 2, the TGA results for 3 different cases studied in this work are represented: 6FDA-6FpDA with 10 wt. % of the 6 different particles, 6FDA-6FpDA with different percentage of the BCZY particles, and 6FDA-6FpDA, Matrimid® and P84® with 10 wt. % of BCZY. It can be appreciated that the temperature of the maximum weight loss ($T_{max\ loss}$) is a characteristic property of the polymer matrix, i.e. 550 ºC for 6FDA-6FpDA, 560 ºC for Matrimid® and, finally, 580 ºC for P84®. The value of the residual mass R_M, determined after exposure of the sample to synthetic air at 800 ºC, theoretically indicates the content of inorganic particles within the sample. However, in the case of the zeolites (ITQ-2 and Beta), it does not behave this way since the nanometer size of the particles may cause loss of part of the constituting elements of these particles. Conversely, for the samples: 6FDA-6FpDA 20 %wt. BCZY, and for Matrimid® 10 wt. % BCZY, R_M is higher than the initial percentage of particles which may indicates an irregular distribution of the polymer chains around the particles. Additionally, an identical temperature of the maximum weight loss $T_{max\ loss}$ for 6FDA-6FpDA with different percentages of the BCZY particles is observed in Figure 2. From these results, it can be concluded that the incorporation of inorganic particles to the polymer matrix does not affect the thermal stability of the polymer.

The glass transition temperature (T_g) of these three polymers was determined by differential scanning calorimetry (DSC). An evolution of the T_g with the rigidity of the polymer chains following the order of rigidity 6FDA-6FpDA< Matrimid® < P84® was found. For all the 6FDA-6FpDA-based MMMs the T_g decreases in comparison to the pure polyimide, except for the BCZY membrane that presents a T_g similar to the reference. The observed reduction of the T_g may indicate a plasticization effect introduced by the filler particles.

When the behavior of the T_g for different BCZY contents in the polymer matrix was analyzed, only small irregular changes were found, *i.e.* an increase of T_g for low BCZY percentages between 1 and 5 wt. % and a slightly higher increase for 10 wt. %, which may indicate an small macromolecular chain rigidification [34] (see Table 2). This could have an effect on the gas transport properties, expecting an increase in selectivity but decrease of the permeability coefficients.

Preprints (www.preprints.org) | NOT PEER-REVIEWED | Posted: 8 November 2018 doi:10.20944/preprints201811.0186.v1

Peer-reviewed version available at Membranes 2018, 8, 128; doi:10.3390/membranes8040128

Table 2. TGA and DSC results for the three different cases studied in this work

	$T_{max\ loss}$	Theor. wt. %	R_M wt. %	T_g
6FDA-6FpDA	550 ºC	0	0	311.1 ºC
+ 10 wt. % 8YSZ	550 ºC	10	9.8	300.2 ºC
+ 10 wt. % La_2O_3	550 ºC	10	8.1	302.4 ºC
+ 10 wt. % LaWO	550 ºC	10	8.1	290.6 ºC
+ 10 wt. % BCZY	550 ºC	10	10.0	311.2 ºC
+ 10 wt. % ITQ-2	550 ºC	10	0	294.7 ºC
+ 10 wt. % Beta	550 ºC	10	0	294.5 ºC
6FDA-6FpDA	550 ºC	0	0	311.1 ºC
+ 1 wt. % BCZY	550 ºC	1	0	314.2 ºC
+ 5 wt. % BCZY	550 ºC	5	4.9	312.5 ºC
+ 10 wt. % BCZY	550 ºC	10	10.0	311.2 ºC
+ 15 wt. % BCZY	550 ºC	15	16.8	307.9 ºC
+ 20 wt. % BCZY	550 ºC	20	27.2	306.3 ºC
6FDA-6FpDA	550 ºC	0	0	311.1 ºC
+ 10 wt. % BCZY	550 ºC	10	10.0	311.2 ºC
Matrimid®	560 ºC	0	0	320.2 ºC
+ 10 wt. % BCZY	560 ºC	10	13.3	315.7 ºC
P84®	580 ºC	0	0	322.4 ºC
+ 10 wt. % BCZY	580 ºC	10	7.2	318.2 ºC

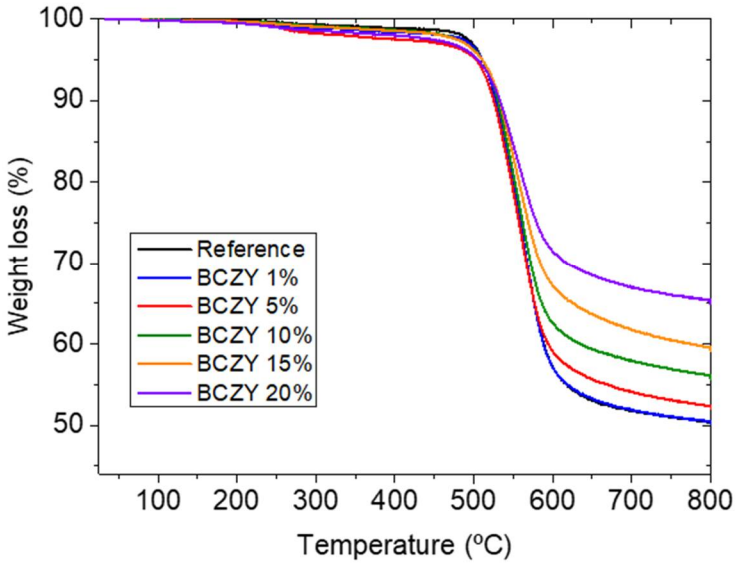

Figure 2. TGA graphs for the results of 6FDA-6FpDA with different percentage of the BCZY particles

2. Microstructure characterization

The X-ray diffraction (XRD) technique is used to evaluate how the particles used in this work interact with the polymer matrix. Figure 3 shows the X-ray spectra of the MMMs with 10 wt. % of particles. In addition, reference patterns of 8YSZ, $La(OH)_3$, LaWO and BCZY crystals are shown. Regarding La_2O_3, this inorganic filler is highly hygroscopic, which may affect its crystalline structure. Actually, this was the case in this work, and, as revealed in Figure 3, the pattern of La_2O_3 changed to $La(OH)_3$. Nonetheless, all these results demonstrate that the particles are well integrated in the polymer matrix, showing the combination of the diffraction pattern of the polymer and particles. Nevertheless, in the case of 8YSZ, La_2O_3 and Beta zeolite, the main peak of the polymer matrix moves to higher values of 2Θ and, therefore, the polymer intersegmental distance decreases [35-37]. This may indicate that part of the fraction free volume (FFV) of the polymer can be altered in the vicinity to the embedded particle.

Figure 4 displays the X-ray diffraction pattern of MMMs made of 6FDA-6FpDA, Matrimid® and P84® combined with BCZY 10 wt. % and illustrates how the intersegmental distance between polymer backbones are directly related to the FFV (6FDA-6FpDA > Matrimid® > P84®) [38, 39].

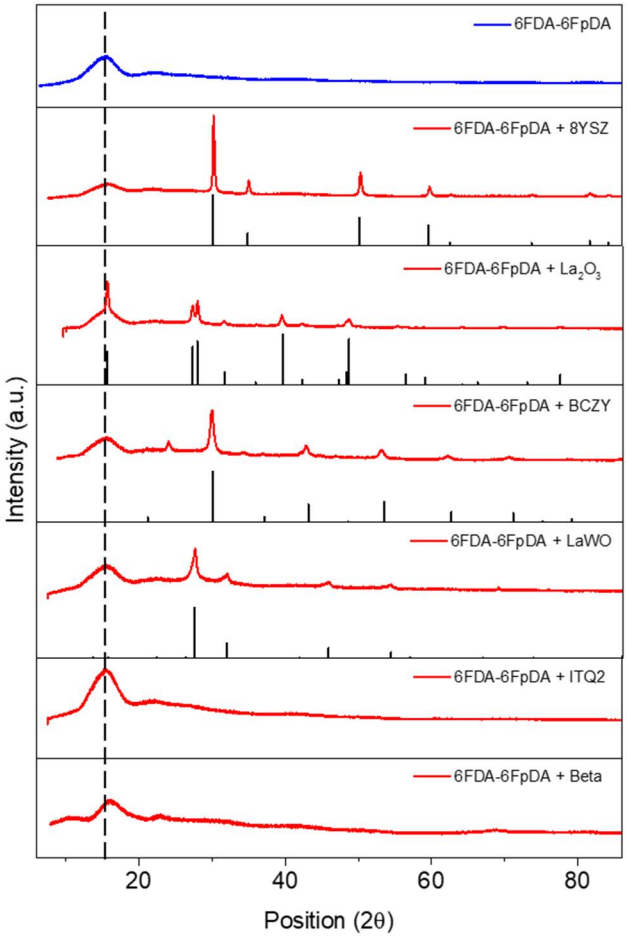

Figure 3. X-ray diffraction patterns for 6FDA-6FpDA with 10 %wt. fillers (red lines) and reference patterns corresponding to 8YSZ, $La(OH)_3$, LaWO and BCZY crystals (black peaks)

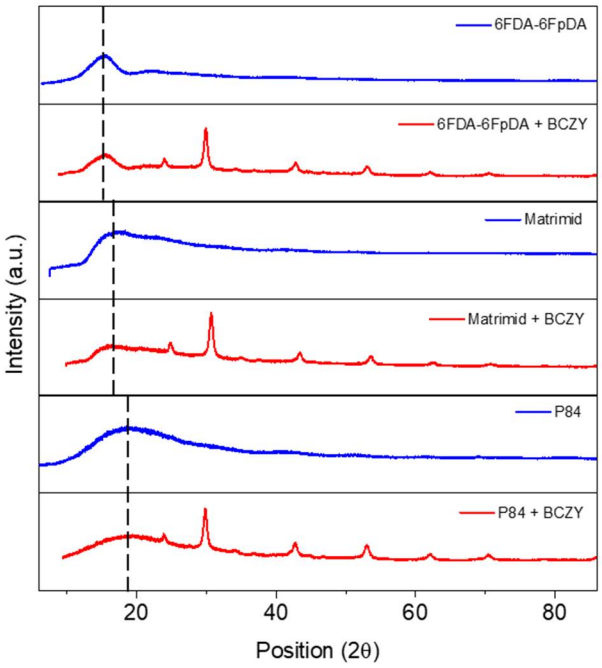

Figure 4. X-ray patterns for different polymer matrix: pure – blue lines, and with 10 %wt. BCZY – red lines

The fillers distribution, sedimentation and agglomeration in the membranes were analyzed based on SEM cross-sectional images.

The cross-section of 6FDA-6FpDA MMMs with 10 %wt. fillers (Figure 5) shows that part of the inorganic fillers forms agglomerates. Theoretically, the size of particles (Table 1) should be in the nanometer range, but most of the fillers occur as agglomerates of embedded single nanoparticles. Additionally, sedimentation of particles can also be appreciated, i.e. there is a certain sedimentation for most fillers. These two phenomena may be associated with the dynamics of the membrane formation process. In general, the process for solvent evaporation is slow, and it gives enough time for particles for sedimentation to the bottom, which is something very common in thick films MMMs. This is related to the solvent used, NMP, that exhibits a high boiling point and to the high density of most of the studied filler particles (Table 1). When all the inorganic fillers are compared, it is ascertained that La_2O_3 showed the largest amount of agglomerates and, in general, a poor distribution. In contrast, BCZY is the filler with best particle distribution throughout the membrane thickness, the least agglomeration and sedimentation.

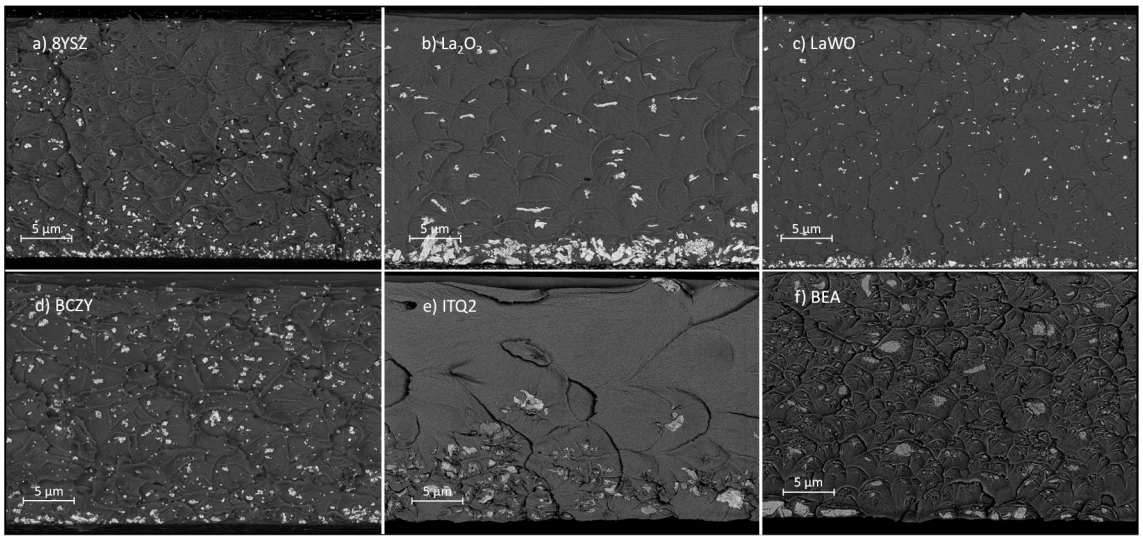

Figure 5. SEM images (fracture cross-sections) for 6FDA-6FpDA MMM and 10 wt. % fillers

3. Gas transport properties

In this section, the gas transport properties for the three different cases (*i.e.* particle type, particle content and polymer type) are evaluated. Time lag equipment was used to study, not only the permeability and the selectivity, but also the solubility and the diffusivity coefficients of gases and water vapor in MMMs as a function of temperature.

a. Influence of the particle type

In this section, MMMs composed by 90 wt. % of 6FDA-6FpDA as polymer matrix and 10 wt. % of different fillers are characterized Table 3 shows how the particles influence the polymer matrix reference (6FDA-6FpDA) in terms of permeability and selectivity at 30 ºC. Permeability variations are always negative and, on the contrary, the selectivity variations are positive in all the cases. The decrease in permeability with the addition of inorganic fillers can be related to the formation of a densified layer of polymer on the polymer/particle interphase, although a reduction of the T_g was not observed (Table 2). Polymer densification leads to reduced free volume and, consequently, to higher selectivity for the gas pair with significantly different kinetic diameters of gas molecules. Interestingly, the decrease in CO_2 permeability leads to significant, reverse-proportional increase of the activation energy of CO_2 permeability [40]. This observation allows one to conclude about good contact between polymer and inorganic particle, i.e. presence of no gaps in this interface [10, 41].

Preprints (www.preprints.org) | NOT PEER-REVIEWED | Posted: 8 November 2018 doi:10.20944/preprints201811.0186.v1

Peer-reviewed version available at Membranes 2018, 8, 128; doi:10.3390/membranes8040128

Table 3. CO_2 permeability, CO_2/CH_4 selectivity, percentage variations of permeability and selectivity (6FDA-6FpDA with 10 wt. %fillers at 30 °C). Additionally, the activation energy for CO_2 permeability derived from the data shown in Figure 6 is listed.

Membrane sample description	*CO_2 Permeability (Barrer)*	*CO_2/CH_4 Selectivity (-)*	*CO_2 Permeability variation (%)*	*CO_2/CH_4 Selectivity variation (%)*	*Activation energy (KJ/mol)*
6FDA-6FpDA (Reference)	77.4	48.0	-	-	0.69
+ 10 wt. % 8YSZ	25.8	53.9	-67	+12	3.73
+ 10 wt. % La_2O_3	34.1	51.9	-56	+8	2.69
+ 10 wt. % LaWO	11.9	77.3	-85	+61	5.51
+ 10 wt. % BCZY	63.8	54.6	-18	+14	1.22
+ 10 wt. % ITQ-2	28.9	55.1	-63	+15	2.63
+ 10 wt. % Beta	22.7	64.9	-71	+35	4.98

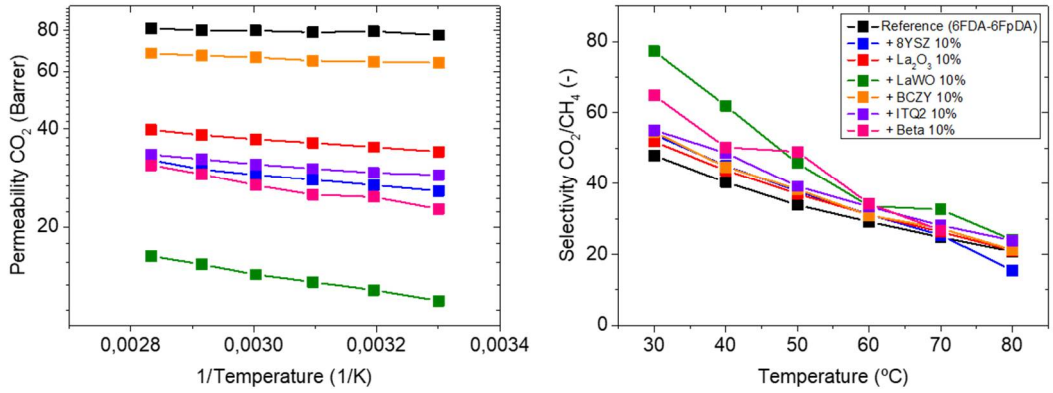

Figure 6. Permeability of CO_2 and CO_2/CH_4 selectivity for the MMM composed by 90 wt. % of 6FDA-6FpDA and 10 wt. % of different fillers as a function of temperature.

The permeability of CO_2 and selectivity for the gas pair CO_2/CH_4 was also measured as a function of temperature. CO_2 permeability increases with temperature for all tested MMMs. However, none of them exhibits higher permeability values than the reference membrane as it is observed in Figure 6 (left-hand). Selectivity decreases as a function of temperature while effect of the type of filler becomes more visible at lower temperatures. Table 3 displays the activation energy for the different fillers and the reference. The activation energy of the MMMs is higher than the activation energy of the polymeric membrane 6FDA-6FpDA. Hence, the formation of a rigid layer around the particles is confirmed.

Taking into consideration all the MMMs, the sample with BCZY particle exhibits the highest permeability value, as well as a notable increase in CO_2/CH_4 selectivity. All MMMs exhibit worse permeability than the reference while a visible improvement in selectivity can be ascertained. Gas

Peer-reviewed version available at Membranes 2018, 8, 128; doi:10.3390/membranes8040128

permeability through a membrane depends on two parameters, diffusivity coefficient and solubility coefficient (Figure 7). The solubility coefficient was not improved by the incorporation of particles. In particular, the membranes containing BCZY and La_2O_3 particles have practically the same CO_2 solubility coefficient as the pure polymer, but the rest of inorganic fillers causes a CO_2 solubility coefficient decrease, and all of them decrease as a function of temperature.

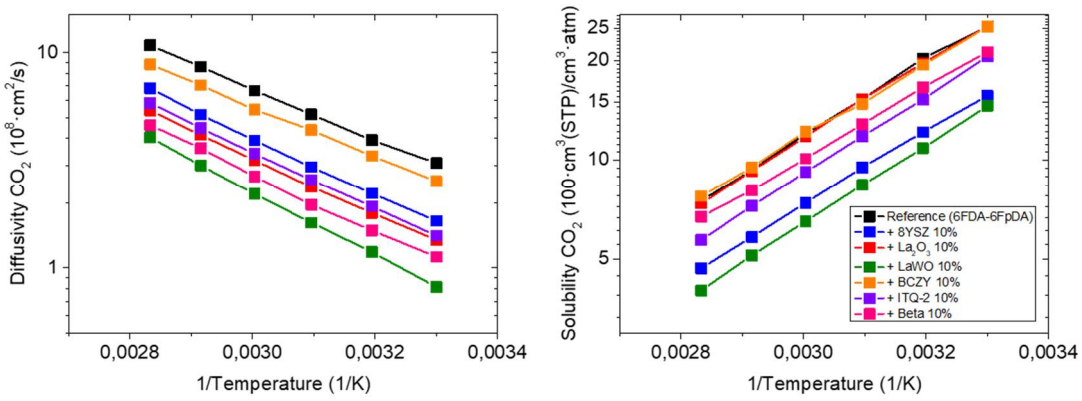

Figure 7. Diffusivity and solubility coefficient of MMMs composed by 90 wt. % of 6FDA-6FpDA and 10 wt. % of different fillers, as a function of temperature

On the contrary, the diffusivity coefficient, which is mainly determined by the FFV, increases as a function of temperature for all the MMMs. It is assumed that particles are blocking part of the FFV of the polymer matrix, and hence, the final permeability decreases. Observing the evolution of the diffusivity coefficient with temperature, this statement can be confirmed, since the reference diffusivity coefficient is higher than the rest at room temperature, and this difference is bigger at higher temperatures.

As a conclusion, BCZY was the most promising particle for MMM and, therefore, this nano-sized filler was selected for the next step, i.e. evaluation of the influence of the amount of nanoparticles on the separation performance.

b. Influence of the particle content

In order to understand the influence of the inorganic filler concentration on MMM transport properties, membranes were prepared with different BCZY content: 1-5-10-15-20 wt. % in the same polymer matrix, *i.e.* 6FDA-6FpDA. Table 4 summarizes permeability and ideal selectivity data obtained for the aforementioned membranes at 30 °C.

As in the previous section, the permeability values for the different filler concentration are lower than the permeability of the reference membrane (6FDA-6FpDA). In contrast, regarding the selectivity variation, the MMM with the highest content of particles has a negative effect on

selectivity. This suggests that not only the filler particles are blocking the FFV -decreasing the permeability- but also aggregates influence the selectivity negatively.

Table 4. CO_2 permeability, CO_2/CH_4 selectivity, percentage variations of permeability and selectivity (6FDA-6FpDA with different % of BCZY at 30 °C). Additionally, the activation energy for CO_2 permeability derived from permeability vs. temperature data is listed.

Membrane sample description	***CO_2 Permeability (Barrer)***	***CO_2/CH_4 Selectivity (-)***	***CO_2 Permeability variation (%)***	***CO_2/CH_4 Selectivity variation (%)***	***Activation energy (KJ/mol)***
6FDA-6FpDA (Reference)	77.4	48.0	-	-	0.69
+ 1% wt. BCZY	61.4	49.7	-21	+3.6	2.56
+ 5% wt. BCZY	45.5	49.6	-41	+3.3	1.89
+ 10% wt. BCZY	63.8	54.6	-18	+14	1.22
+ 15% wt. BCZY	66.0	47.8	-15	-0.3	0.57
+ 20% wt. BCZY	59.7	45.1	-23	-6.0	1.46

Permeability of CO_2 and selectivity of the gas pair CO_2/CH_4 was measured as a function of temperature. Activation energies for the MMMs of 6FDA-6FpDA with different % of BCZY filler are indicated in Table 4. Permeability of CO_2 increases with temperature but decreases with the content of BCZY fillers. All the membranes with BCZY exhibit higher permeability values than with the other fillers studied in the previous section (see Figure 6). This fact indicates that BCZY is the most promising particle. Regarding the selectivity of CO_2/CH_4, it decreases as a function of temperature, and there is not a wide difference between the reference polymer and MMMs. No clear dependence between BCZY content and activation energy can be observed. Therefore, in the next sub-section, the filler BCZY at 10 wt. % is tested for two other polymers that present lower FFV, that is, with, lower permeability, in order to check if the addition of particles enables to improve their separation performance.

c. Influence of the polymer matrix

The influence of different polymeric matrices with different FFV (6FDA-6FpDA, Matrimid® and P84®) on the separation properties is studied, employing the results of the previous studies, that is, the most suitable filler (BCZY) and the most suitable proportion (10 wt. %) [42]. Table 5 shows the polymer matrix influence (6FDA-6FpDA, Matrimid® and P84®) in terms of permeability and selectivity at 30 ºC. We hypothesized that, for lower permeable polymers, the particles may affect positively the gas separation properties of the mixed matrix membranes. As it is shown in the table below, the Matrimid® mixed matrix membrane exhibits higher permeability, as well as selectivity, compared to its reference, while the P84® mixed matrix membrane behaves similar to

Peer-reviewed version available at Membranes 2018, 8, 128; doi:10.3390/membranes8040128

the 6FDA-6FpDA mixed matrix membrane, with a decrease in permeability and an increase in selectivity [41].

Table 5. CO_2 permeability, CO_2/CH_4 selectivity, percentage variations of permeability and selectivity (membranes with different polymeric matrix at 30 °C). Additionally, activation energy is calculated.

Membrane sample description	***CO_2 Permeability (Barrer)***	***CO_2/CH_4 Selectivity (-)***	***CO_2 Permeability variation (%)***	***CO_2/CH_4 Selectivity variation (%)***	***Activation energy (KJ/mol)***
6FDA-6FpDA (Reference)	77.4	48.0	-	-	0.69
+ 10% wt. BCZY	63.8	54.6	-18	+14	1.22
Matrimid®	5.1	40.5	-	-	9.30
+ 10% wt. BCZY	6.7	47.5	+31	+17	7.42
P84®	1.4	47.0	-	-	11.64
+ 10% wt. BCZY	1.0	64.6	-32	+38	18.33

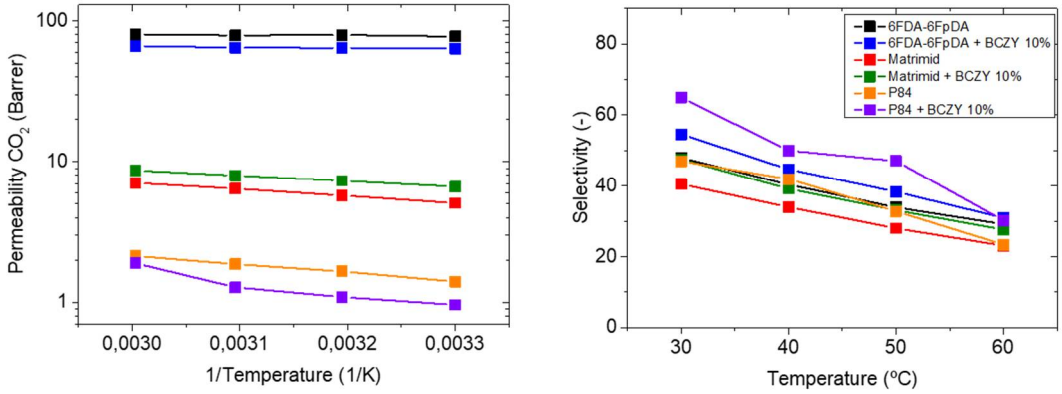

Figure 8. Permeability of CO_2 and CO_2/CH_4 selectivity for the membranes made of 6FDA-6FpDA, Matrimid® and P84® with and without 10 wt. % BCZY as a function of temperature.

The permeability of CO_2 and the selectivity of the CO_2/CH_4 gas pair were determined as a function of temperature. All polymers show good compatibility with BCZY particles, but behave differently as casted MMMs. 6FDA-6FpDA and P84® show lower permeability coefficients of CO_2 in MMM form while Matrimid® with 10 wt. % of BCZY shows an improvement in both CO_2 permeability and CO_2/CH_4 selectivity. As it can be expected for the CO_2/CH_4 gas pair, the ideal selectivity decreases with temperature for both pure polymer and MMMs.

Figure 9 shows diffusion and solubility coefficients of CO_2 as a function of temperature. It can be ascertained that, the permeability of Matrimid® with BCZY particles is higher than the pure polymer Matrimid® because both, diffusivity and, especially, solubility coefficients improve. In general, the activation energy of CO_2 diffusivity (Figure 9) of the polymer membrane is not

Preprints (www.preprints.org) | NOT PEER-REVIEWED | Posted: 8 November 2018 doi:10.20944/preprints201811.0186.v1

Peer-reviewed version available at Membranes 2018, 8, 128; doi:10.3390/membranes8040128

influenced by the incorporation of BCZY particles suggesting that the diffusion mechanism is apparently not affected.

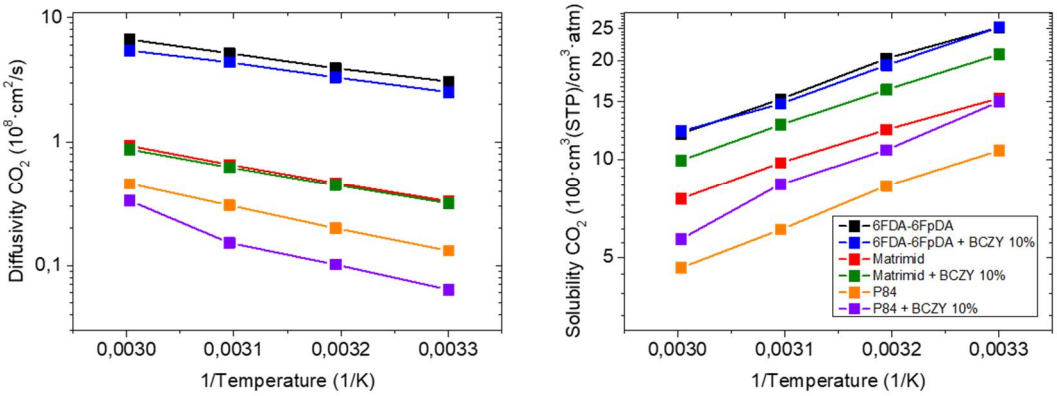

Figure 9. Diffusivity and solubility coefficient of CO_2 of membranes made of 6FDA-6FpDA, Matrimid® and P84® with and without 10 wt. % BCZY as a function of temperature

d. Transport of water vapor in MMMs

The fillers selected for this work exhibit a high affinity towards water. They can be perspective materials for membranes able to remove water from CO_2-rich gas streams as combustion tail-gas or catalytic converters products. Additionally, all the MMMs tested until now exhibits high CO_2 solubility coefficients, which may be related with to the water vapor transport properties. Hence, all prepared membranes were tested for water vapor transport using the "time-lag" setup.

Table 6 summarizes water vapor permeabilities and the activation energies for all the MMMs studied in this work. The achieved permeability values are remarkably high, although permeability decreases as a function of temperature. The negative values of the activation energy are related to the exothermic nature of the water solubility and its effect dominates in the overall separation process. In all cases, water permeability decreased in MMMs compared to pure polymers except the case of Matrimid® with 10 wt. % of BCZY. This filler showed the highest permeability coefficient of MMMs when compared to other fillers mixed with 6FDA-6FpDA. Looking at activation energies of water permeability in 10 wt. % MMMs based on three polymers, one may conclude that the "slower" polymers Matrimid® and P84® are more benefitting by the incorporation of BCZY. Namely, P84®-based MMM shows slightly positive E_a (P) for water vapor and Matrimid® MMM exhibits a higher water permeability coefficient than for the pure polymer and a lower corresponding activation energy. These two materials are appealing materials for further application in membrane-assisted water vapor removal from combustion streams or in catalytic reactors in order to shift chemical equilibrium in CO_2-hydrogenation reactions.

Table 6. Steam permeation at 30 °C and activation energies for all the MMMs studied in this work at 30 ºC.

	H_2O permeability (Barrer)	***H_2O/CO_2 Selectivity (-)***	***Activation energy (KJ/mol)***
6FDA-6FpDA	3875	50.06	-3.34
+ 10 wt. %8YSZ	1998	77.48	-2.22
+ 10 wt. %La_2O_3	2381	69.85	-2.79
+ 10 wt. %LaWO	1287	108.30	-1.35
+ 10 wt. %BCZY	3319	52.02	-3.31
+ 10 wt. %ITQ-2	2015	69.70	-1.31
+ 10 wt. %Beta	1914	84.35	0.69
6FDA-6FpDA	3875	50.06	-3.34
+ 1 wt. %BCZY	3144	51.20	-2.30
+ 5 wt. %BCZY	2766	60.83	-2.23
+ 10 wt. %BCZY	3319	52.02	-3.31
+ 15 wt. %BCZY	3276	49.67	-2.13
+ 20 wt. %BCZY	3108	52.03	-2.28
6FDA-6FpDA	3875	50.06	-3.34
+ 10 wt. %BCZY	3319	52.02	-3.31
Matrimid®	1524	300.60	0.87
+ 10 wt. %BCZY	1835	276.02	-1.16
P84®	1226	875.71	2.36
+ 10 wt. %BCZY	821	856.40	1.73

Conclusions

A complete study of the influence of inorganic fillers on the gas transport properties of different polyimides, typically applied in gas separation processes, *i.e.* purification of biogas and natural gas was developed. The strategy of this work was the incorporation of inorganic nanoparticles as MMM fillers. These inorganic materials were selected because the expected good affinity for gas molecules as CO_2 and water vapor. The particles were successfully dispersed and incorporated into the polymer matrix. Consequently, 15 different MMMs were produced as a thick film. Materials were characterized by different techniques including TGA, XRD, DSC or SEM. Gas transport properties were evaluated for CH_4, CO_2 and H_2O at temperatures from 30 to 80 °C, in a time lag equipment.

It was observed that, in general, the inorganic fillers could produce small rigidification in the polymer matrix, although they do not exhibit higher T_g. MMMs studied in this work allowed to improve selectivity but with a negative impact on permeability. This could be caused by particle aggregation (see Figure 5 for SEM images), blocking part of the FFV but increasing tortuosity of

the gases trough the membrane. Regarding the influence of the particle type and/or content, no clear effect of the particles in terms of pore size or particle size was discovered. XRD analysis shows a small decrease in interspacing of the polymer chains with no modification of the particles pattern, meaning that there is not any interaction with polymer.

Taking all the inorganic particles into consideration, BCZY shows the best improvement of selectivity with a small decrease in permeability. In addition, it also exhibits the best distribution and, consequently, it was selected for the rest of the experiments (different percentages and different polymer matrix). For polymer matrixes with lower FFV, such as Matrimid® and P84®, there is a result in improvement of the properties by adding particles, possible due to the creation of interface between particle and polymer chain. Therefore, MMMs with particles can be used to create interface and we will increase separation properties of slow polymers. Regarding temperature dependence, some changes were observed on activation energy of the process, the incorporation of inorganic fillers does not significantly affect the permeation mechanism determined by the polymer transport properties.

Finally, water permeability was firstly reported for several polyimides and MMMs of inorganic particles with polyimides, reaching relatively high values. However, the effect of the filler incorporation on the water permeation was not relevant for the polymers except for Matrimid.

Acknowledgements

This work was financially supported by the Spanish Government (SEV-2016-0683, SVP-2014-068356, Project ENE2014-57651-R and IJCI-2016-28330 grants) and Generalitat Valenciana (PROMETEO/2018/006 grant).

Authors are grateful to Susana Valencia (Instituto de Tecnología Química (UPV-CSIC)) for zeolite synthesis; Clarissa Abetz and Anke-Lisa Hoeme (Helmholtz-Zentrum Geesthacht) for excellent SEM images; Silvio Neumann (Helmholtz-Zentrum Geesthacht) for the TGA and DSC measurements and Giovanni Capurso (Helmholtz-Zentrum Geesthacht) for the XRD measurements.

References

1. Santi Kulprathipanja, R.W.N., Norman N. Li *Separation of fluids by means of mixed matrix membranes*. 1988, Honeywell International Inc
2. Kulprathipanja, S., *Mixed Matrix Membrane Development.* Annals of the New York Academy of Sciences, 2003. **984**(1): p. 361-369.
3. Robeson, L.M., *The upper bound revisited.* Journal of Membrane Science, 2008. **320**(1): p. 390-400.
4. Paul, D.R. and U.P. Yampolskij, *Polymeric gas separation membranes*. 1994, Boca Raton: CRC.

5. Baker, R.W., *Research needs in the membrane separation industry: Looking back, looking forward.* Journal of Membrane Science, 2010. **362**(1): p. 134-136.
6. Stünkel, S., et al., *Carbon dioxide capture for the oxidative coupling of methane process – A case study in mini-plant scale.* Chemical Engineering Research and Design, 2011. **89**(8): p. 1261-1270.
7. Cheng, Y., Z. Wang, and D. Zhao, *Mixed Matrix Membranes for Natural Gas Upgrading: Current Status and Opportunities*. Vol. 57. 2018.
8. J. Koros, W. and C. Zhang, *Materials for next-generation molecularly selective synthetic membranes*. Vol. 16. 2017.
9. Li, Y., et al., *Recent advances in the fabrication of advanced composite membranes*. Vol. 1. 2013.
10. Bastani, D., N. Esmaeili, and M. Asadollahi, *Polymeric mixed matrix membranes containing zeolites as a filler for gas separation applications: A review.* Journal of Industrial and Engineering Chemistry, 2013. **19**(2): p. 375-393.
11. Carreon, M.A., *Membranes for gas separations.* 2018.
12. Liu, C., D.W. Greer, and B.W. O'Leary, *Advanced Materials and Membranes for Gas Separations: The UOP Approach*, in *Nanotechnology: Delivering on the Promise Volume 2*. 2016, American Chemical Society. p. 119-135.
13. Dechnik, J., et al., *Mixed-Matrix Membranes.* Angewandte Chemie International Edition, 2017. **56**(32): p. 9292-9310.
14. Yang, Y., et al., *Enhancing the mechanical strength and CO_2/CH_4 separation performance of polymeric membranes by incorporating amine-appended porous polymers.* Journal of Membrane Science, 2019. **569**: p. 149-156.
15. Mikkelsen, M., M. Jørgensen, and F.C. Krebs, *The teraton challenge. A review of fixation and transformation of carbon dioxide.* Energy & Environmental Science, 2010. **3**(1): p. 43-81.
16. Miltner, M., A. Makaruk, and M. Harasek, *Review on available biogas upgrading technologies and innovations towards advanced solutions.* Journal of Cleaner Production, 2017. **161**: p. 1329-1337.
17. Ullah Khan, I., et al., *Biogas as a renewable energy fuel – A review of biogas upgrading, utilisation and storage.* Energy Conversion and Management, 2017. **150**: p. 277-294.
18. Montañez-Hernández, L., et al., *Sustainable Production of Biogas from Renewable Sources: Global Overview, Scale Up Opportunities and Potential Market Trends*. 2018. 325-354.
19. Baker, R.W. and K. Lokhandwala, *Natural Gas Processing with Membranes: An Overview.* Industrial & Engineering Chemistry Research, 2008. **47**(7): p. 2109-2121.
20. Zhang, Y., et al., *Current status and development of membranes for CO_2/CH_4 separation: A review.* International Journal of Greenhouse Gas Control, 2013. **12**: p. 84-107.
21. Rezakazemi, M., et al., *State-of-the-art membrane based CO_2 separation using mixed matrix membranes (MMMs): An overview on current status and future directions.* Progress in Polymer Science, 2014. **39**(5): p. 817-861.
22. Angelidaki, I., et al., *Biogas upgrading and utilization: Current status and perspectives.* Biotechnol Adv, 2018. **36**(2): p. 452-466.
23. Kanehashi, S., et al., *The impact of water vapor on CO_2 separation performance of mixed matrix membranes.* Journal of Membrane Science, 2015. **492**: p. 471-477.
24. Tena, A., et al., *Influence of the Composition and Imidization Route on the Chain Packing and Gas Separation Properties of Fluorinated Copolyimides.* Macromolecules, 2017. **50**(15): p. 5839-5849.
25. Escorihuela, S., et al., *Gas Separation Properties of Polyimide Thin Films on Ceramic Supports for High Temperature Applications.* Membranes, 2018. **8**(1): p. 16.

26. Corma, A., et al., *Preparation, characterisation and catalytic activity of ITQ-2, a delaminated zeolite.* Microporous and Mesoporous Materials, 2000. **38**(2): p. 301-309.
27. Itoh, T., et al., *Effect of Annealing on Crystal and Local Structures of Doped Zirconia Using Experimental and Computational Methods.* The Journal of Physical Chemistry C, 2015. **119**(16): p. 8447-8458.
28. Vigneron, F., et al., *Etude par diffraction de neutrons des structures magnétiques de TbBe 13 à basse température.* Journal de Physique, 1980. **41**(2): p. 123-133.
29. Scherb, T., et al., *Nanoscale order in the frustrated mixed conductor La5.6WO12-[delta].* Journal of Applied Crystallography, 2016. **49**(3): p. 997-1008.
30. Han, D., et al., *A Comprehensive Understanding of Structure and Site Occupancy of Y in Y-Doped $BaZrO_3$.* Journal of Materials Chemistry A, 2013. **1**: p. 3027-3033.
31. Morejudo, S.H., et al., *Direct conversion of methane to aromatics in a catalytic co-ionic membrane reactor.* Science, 2016. **353**(6299): p. 563-566.
32. *IZA Structure Comission*. 2018; Available from: http://www.iza-structure.org/.
33. Zhang, C., et al., *High performance ZIF-8/6FDA-DAM mixed matrix membrane for propylene/propane separations.* Journal of Membrane Science, 2012. **389**: p. 34-42.
34. Sabetghadam, A., et al., *Metal Organic Framework Crystals in Mixed-Matrix Membranes: Impact of the Filler Morphology on the Gas Separation Performance.* Advanced Functional Materials, 2016. **26**(18): p. 3154-3163.
35. Khayet, M. and M.C. García-Payo, *X-Ray diffraction study of polyethersulfone polymer, flat-sheet and hollow fibers prepared from the same under different gas-gaps.* Desalination, 2009. **245**(1): p. 494-500.
36. Recio, R., et al., *Gas separation of 6FDA–6FpDA membranes: Effect of the solvent on polymer surfaces and permselectivity.* Journal of Membrane Science, 2007. **293**(1): p. 22-28.
37. Tylkowski, N.A.G.B.a.B., *Chemical Synergies: From the Lab to In SIlico Modelling*. 2018: De Gruyter.
38. Calle, M., et al., *Design of gas separation membranes derived of rigid aromatic polyimides. 1. Polymers from diamines containing di-tert-butyl side groups.* Journal of Membrane Science, 2010. **365**(1): p. 145-153.
39. Liu, Y., et al., *Barrier and thermal properties of polyimide derived from a diamine monomer containing a rigid planar moiety.* Polymer International, 2017. **66**(8): p. 1214-1222.
40. Yampolskii, Y., et al., *Correlations with and prediction of activation energies of gas permeation and diffusion in glassy polymers.* Journal of Membrane Science, 1998. **148**(1): p. 59-69.
41. Jamil, A., P.C. Oh, and A. B. M. Shariff, *Current Status and Future Prospect of Polymer-Layered Silicate Mixed-Matrix Membranes for CO_2/CH_4 Separation*. Vol. 39. 2016.
42. Bae, T.-H. and J.R. Long, *CO_2/N_2 separations with mixed-matrix membranes containing Mg2(dobdc) nanocrystals.* Energy & Environmental Science, 2013. **6**(12): p. 3565-3569.